

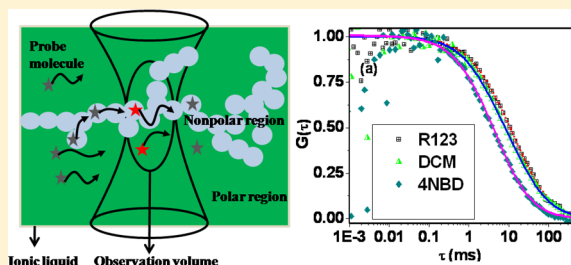
# Microheterogeneity of Some Imidazolium Ionic Liquids As Revealed by Fluorescence Correlation Spectroscopy and Lifetime Studies

Satyajit Patra and Anunay Samanta\*

School of Chemistry, University of Hyderabad, Hyderabad 500046, India

## S Supporting Information

**ABSTRACT:** The microscopic structure and dynamics of the room temperature ionic liquids (RTILs) that are responsible for some of the peculiar properties of this class of solvents continue to intrigue the researchers and stimulate new investigations. Herein, we use the fluorescence correlation spectroscopy (FCS) technique to study the diffusion of some probe molecules in RTILs, the results of which, when combined with those obtained from fluorescence lifetime studies, provide insights into the microscopic structural details of this class of novel solvents. Experiments performed with three charged and neutral probe molecules in five carefully selected 1-alkyl-3-methylimidazolium ionic liquids reveal that unlike in conventional solvents these probes exhibit a bimodal diffusion behavior in RTILs thus indicating the presence of two distinct environments. It is found that the contribution of the slow component of the diffusion increases with increasing alkyl chain length of the cation. Not only are these results supported by the biexponential decay behavior of the fluorescence intensity of the systems, but the individual values of the lifetime components and their weight allow determination of the nature of the two major environments. In essence, the results point to the potential of the two combined techniques in unraveling some of the complex features of the ionic liquids.



## 1. INTRODUCTION

Room temperature ionic liquids (RTILs) possess some extraordinary properties, such as low vapor pressure, liquidity over a wide range of temperature, high conductivity, high thermal stability, high electrochemical window, moderate to high polarity, and nonflammable nature, which make them useful media for a large number of organic and inorganic reactions, catalysis, separation and energy-related applications, such as fuel cell, photovoltaics, supercapacitors, and batteries.<sup>1–8</sup> It is thus not difficult to understand why these substances have attracted such huge attention in recent years. The fact that it is possible to develop ionic liquids with desirable properties or tune their properties gradually by appropriate selection of the constituent ions makes them “designer solvents” for fundamental studies and applications.

Many experimental and theoretical studies in recent years have indicated that the RTILs are more structured liquids when compared to the conventional solvents.<sup>9–34</sup> This structural heterogeneity of the RTILs, which appears to be responsible for many of the peculiar properties of these substances, is understood to occur over a spatial scale of few nanometers and arises from the segregation of the alkyl tails into the mesoscopic domains.<sup>13,14,16,17,21–26</sup> The early indication of this heterogeneity came through some scattered experiments based on various techniques.<sup>9–12</sup> Notable among those are the observation of the excitation wavelength dependence of the fluorescence behavior of dipolar systems and reaction rates faster than the diffusion.<sup>9–11,19</sup> These experiments did not provide any structural details of these liquids but indicated that

the RTILs are not homogeneous media at the microscopic level. Hamaguchi and co-workers proposed a local ordering in these materials to interpret the Raman spectroscopy data of a few RTILs.<sup>18,34</sup> The spatial heterogeneity in RTILs was subsequently supported by the molecular dynamics (MD) simulation studies by different groups.<sup>13–17</sup> These studies revealed for the first time that the nanoscale organization in RTILs is the consequence of the segregation of the alkyl chains. The first experimental evidence of the spatial heterogeneity of the RTILs and its scale came from small wide-angle X-ray scattering (SWAXS) experiments.<sup>21–27</sup> However, recent neutron scattering and computational studies question some of the conclusions of the SWAXS study.<sup>35,36</sup> Thus it appears that the structure of the RTILs is yet to be fully understood, and it requires further experiments and simulation to unravel some of the details of the local structure and dynamics. Russina et al. present the current understanding of the mesoscopic structural heterogeneity of the RTILs in two very recent articles.<sup>25,26</sup>

Fluorescence correlation spectroscopy (FCS) is a highly sensitive and powerful technique for the study of diffusion of molecular systems in a medium. In this technique, one measures the fluctuations of the fluorescence intensity in a highly dilute solution arising from a small excitation volume (approximately 1 fL) defined by the focused laser beam and

Received: June 21, 2012

Revised: August 23, 2012

Published: October 2, 2012

pinhole.<sup>37</sup> These fluctuations are correlated to generate the correlation function. The decay of this correlation function with time contains information on the dynamic molecular processes responsible for the fluorescence fluctuation, e.g., translational diffusion, conformation fluctuation, reaction kinetics, etc.<sup>37</sup> This technique has been used to study blinking dynamics, bimolecular reaction, conformation fluctuation, and translational diffusion in organized assembly like polymer, lipid, membranes, etc.<sup>38–41</sup> A few FCS studies in neat RTILs and in solutions have been carried out to understand the diffusion behavior of molecular systems in these media.<sup>42–45</sup> Werner et al. were the first to study the diffusion behavior of some probe molecules using FCS measurements in a RTIL.<sup>42</sup> Apart from demonstrating the usefulness of the technique in probing the frictional resistance experienced by the molecules, the extent of solvent association of the probe molecules in RTILs was estimated.<sup>42</sup> Bhattacharyya and co-workers observed an unusually broad distribution of the diffusion coefficients of some fluorescent probe molecules in RTILs, which they attributed to the microheterogeneity of ionic liquids.<sup>43</sup> In a more recent FCS study, Guo et al. observed biphasic diffusion dynamics of rhodamine 6G in a series of pyrrolidinium ionic liquids comprising different alkyl chain lengths.<sup>44</sup> They observed an increase in the relative contribution of the slow diffusion component with increasing alkyl chain length, and this finding was ascribed to the increase in the size of aggregated domains formed by the alkyl tails of the cationic group. These are very interesting findings, which, however, require further investigations as the experiments have so far been conducted only on a very few select ionic liquids employing a few fluorescent probes. This is why we undertake this present study in which we employ three carefully chosen fluorescent dyes, R123 (cationic), DCM (neutral), and 4NBD (neutral) to probe the microscopic structure and dynamics in five carefully selected 1-alkyl-3-methylimidazolium ionic liquids. Moreover, we carry out parallel fluorescence lifetimes studies of these three environment sensitive probe molecules<sup>46–49</sup> to supplement the results of the FCS measurements, to understand the structural origin of this bimodal diffusion behavior, and to obtain a more compelling evidence of the structural heterogeneity of the ionic liquids. A total of five ionic liquids have been chosen for this study. The first two ionic liquids contain a common 1-butyl-3-methylimidazolium cation, represented here as [Bmim]<sup>+</sup>, and two different anions, BF<sub>4</sub><sup>−</sup> and PF<sub>6</sub><sup>−</sup>. The three other ionic liquids comprise a common bis(trifluoromethanesulfonyl)imide [Tf<sub>2</sub>N]<sup>−</sup> anion and 1-alkyl-3-methylimidazolium [C<sub>*n*</sub>mim]<sup>+</sup> cations with an alkyl chain length *n* = 2, 4, and 6. Structures of the RTILs and probe molecules are given in Charts 1 and 2, respectively.

## 2. EXPERIMENTAL SECTION

**2.1. Materials.** Laser grade dye, DCM, was purchased from Exciton Inc. and used as received. R123 was purchased from Aldrich and used as received. 4NBD was prepared following a standard procedure published elsewhere.<sup>46</sup> [Bmim][PF<sub>6</sub>], [Bmim][BF<sub>4</sub>], [Emim][Tf<sub>2</sub>N], [Bmim][Tf<sub>2</sub>N], and [Hmim][Tf<sub>2</sub>N] were of “Advanced Materials Research” grade from Kanto Chemicals (Japan). These ionic liquids were rigorously dried under high vacuum for 48 h prior to use. Ethanol (EtOH) and acetonitrile (ACN) were purchased from Merck and distilled and dried prior to use following standard procedures.<sup>50</sup> All the experiments were carried out at 25 °C. Milli Q water was used in the present study.

Chart 1

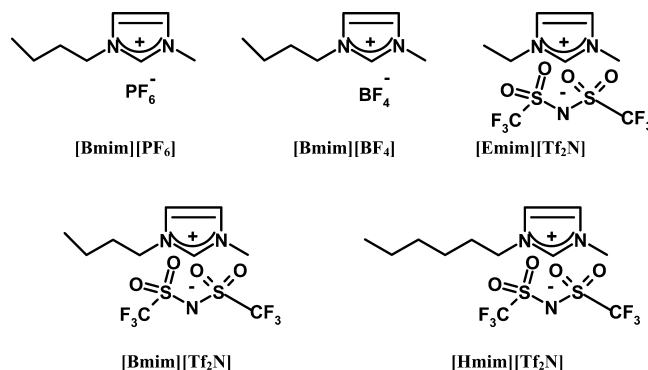
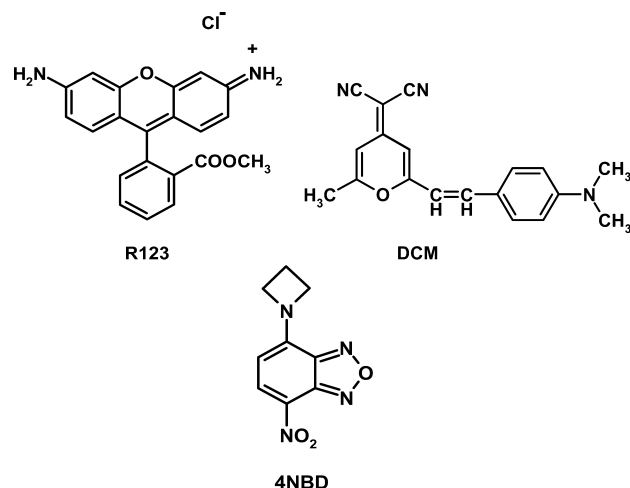


Chart 2



**2.2. Instrumentation.** FCS measurements were performed using a time-resolved confocal fluorescence setup (MicroTime 200, PicoQuant), with an inverted microscope body (Olympus IX 71). The microscope body is equipped with an Olympus UPlansApo NA 1.2 water immersion objective (60×). All the samples were excited at 485 nm with a stable repetition rate of 20 MHz from a pulsed diode laser (PDL 828 S “SEPIA II”, PicoQuant). The output of the pulsed picosecond laser diodes (485 nm, fwhm = 144 ps) was coupled into the main optical unit using a polarization maintaining single-mode optical fiber, guided through a dichroic mirror, and then the collimated laser beam was directed into the entrance port of the inverted microscope. The sample was placed on a coverslip, and the water immersion objective focused the laser beam onto the sample. Fluorescence was collected by the same objective and dichroic mirror, filtered by passing through a 510 nm long-pass filter, and then focused onto a 50 μm diameter pinhole to remove the out-of-focus signals, recollimated, and directed onto a (50/50) beam splitter prior to entering two single-photon avalanche photodiodes (SPADs). The fluorescence correlation traces were generated by cross-correlating signals from the two SPAD detectors. The data acquisition was performed with a PicoHarp 300 TCSPC module in a time-tagged time-resolved (TTTR) mode, which records the arrival times of all photons relative to the beginning of the experiment in addition to TCSPC timing, which measures relative times between a laser excitation pulse and the corresponding fluorescence photon arrival times at the detector. So complete dynamics of the fluorescence intensity is captured.<sup>51</sup> Data analysis of the

individual correlation curves was performed by using the SymPhoTime software of PicoQuant. The correlation function of the fluorescence intensity is given by<sup>37</sup>

$$G(\tau) = \frac{\langle \delta F(t) \delta F(t + \tau) \rangle}{\langle F(t) \rangle^2} \quad (1)$$

where  $\langle F(t) \rangle$  is the average fluorescence intensity and  $\delta F(t)$  and  $\delta F(t + \tau)$  are the deviations from the mean value at time  $t$  and  $(t + \tau)$  and are given by

$$\begin{aligned} \delta F(t) &= F(t) - \langle F(t) \rangle, \\ \delta F(t + \tau) &= F(t + \tau) - \langle F(t) \rangle \end{aligned} \quad (2)$$

The correlation functions were fitted to the following equation<sup>52</sup>

$$G(\tau) = \frac{1}{N} \sum_{i=1}^n \frac{\alpha_i}{\left(1 + \frac{\tau}{\tau_i}\right) \left(1 + \frac{\tau}{\kappa^2 \tau_i}\right)^{1/2}} \quad (3)$$

where  $\alpha_i$  is the fraction of the molecules with a diffusion time of  $\tau_i$ .  $N$  is the average number of fluorescent molecules in the confocal volume.  $\kappa$  is the structure parameter of the observation volume and is given by  $\kappa = \omega_z/\omega_{xy}$ , where  $\omega_z$  and  $\omega_{xy}$  are the longitudinal and transverse radii, respectively, of the confocal volume. The structure parameter of the excitation volume was calibrated by using R6G in water of known diffusion coefficient ( $D_t = 426 \mu\text{m}^2/\text{s}$ ).<sup>53</sup> The estimated excitation volume is 0.8 fL. The  $D_t$  value was calculated using the following equation employing the  $\tau_i$  value obtained from the fit to eq 3.

$$\tau_i = \frac{\omega_{xy}^2}{4D_t} \quad (4)$$

The concentrations of the samples were maintained at  $\sim 35$ – $40$  nM throughout the measurement for good quality signal. The excitation power was  $2 \mu\text{W}$  during the course of the measurement. Low excitation power was used in order to avoid any background fluorescence from ionic liquids. The fluorescence intensity time trace of [Bmim][PF<sub>6</sub>] alone and R123 in [Bmim][PF<sub>6</sub>] is shown in Figure S1 of the Supporting Information. The problem of different refractive index of the ionic liquids and water was addressed by changing the objective collar setting according to the procedure already reported in the literature.<sup>41</sup> Fluorescence lifetime measurements were carried out using a time-correlated single-photon counting (TCSPC) spectrometer (Horiba JobinYvon IBH). Nano LED ( $\lambda_{\text{ex}} = 439$  nm) was used as the excitation source and an MCP photomultiplier (Hamamatsu R3809U-50) as the detector. The pulse repetition rate of the laser source was 1 MHz. The instrument response function, which was limited by the fwhm of the excitation pulse, was 130 ps. The lamp profile was recorded by placing a dilute solution of Ludox in water as a scatterer in place of the sample. Decay curves were analyzed by nonlinear least-squares iteration procedure using IBH DAS6 (Version 2.2) decay analysis software. The quality of the fit was assessed by the  $\chi^2$  values and the distribution of the residuals. The bulk viscosities of the ILs were measured at 25 °C by a LVDV-III Ultra Brookfield Cone and Plate viscometer (1% accuracy and 0.2% repeatability). The measured values are consistent with the literature reports.<sup>20,54,55</sup>

### 3. RESULTS AND DISCUSSION

**3.1. Diffusion in Acetonitrile (ACN)–Ethanol (EtOH) Mixture.** In order to obtain an estimate of the size of the probes in RTILs, the diffusion of the probe molecules is first studied in a ACN–EtOH mixture ( $x_{\text{ACN}} = 0.8$ ) considering the fact that these liquids are more polar than ACN but less polar than MeOH.<sup>56–59</sup> The van der Waals radii ( $R_v$ ) of R123, DCM, and 4NBD, calculated from the van der Waals increments for atoms or groups, are 0.41, 0.40, and 0.34 nm, respectively.<sup>60</sup> Thus R123 and DCM are almost equal in size, and 4NBD is smaller than the other two probes. Correlation curves of the probes in ACN–EtOH mixture ( $x_{\text{ACN}} = 0.8$ ) are shown in Figure 1, and the diffusion coefficients ( $D_t$ ) of the probes

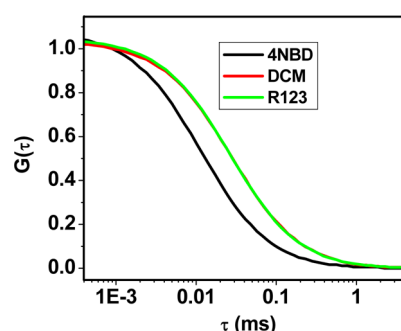


**Figure 1.** Normalized correlation curves for the diffusion of the probes in ACN–EtOH mixture ( $x_{\text{ACN}} = 0.8$ ). The curves shown here are the fits to a single-component diffusion model. The curves for R123 and DCM overlap almost throughout the entire region.

**Table 1.** Diffusion Coefficients ( $D_t$  in  $\mu\text{m}^2\text{s}^{-1}$ ) of the Probes in ACN–EtOH Mixture ( $x_{\text{ACN}} = 0.8$ ) along Their Van der Waals Radius ( $R_v$ ) and Hydrodynamic Radius ( $R$ )

probe	$D_t$	$R_v$ (nm)	$R$ (nm)
4NBD	$1410 \pm 150$	0.34	0.37
DCM	$950 \pm 80$	0.40	0.52
R123	$930 \pm 70$	0.41	0.53

estimated from the data are listed in Table 1. The hydrodynamic radii of the probes are calculated from the Stokes–Einstein equation

$$D_t = \frac{kT}{6\pi\eta R} \quad (5)$$

where  $k$  is the Boltzmann constant,  $T$  is the temperature,  $\eta$  is the viscosity of the medium, and  $R$  is the hydrodynamic radius of the solute molecule. The calculated hydrodynamic radii (Table 1) of R123 and DCM are found to be almost the same (0.53 and 0.52 nm, respectively) in ACN–EtOH mixture ( $x_{\text{ACN}} = 0.8$ ), while that for 4NBD is significantly smaller (0.37 nm). A comparison of the van der Waals and hydrodynamic radii of the molecules suggests a greater degree of solvent association of R123 and DCM compared to 4NBD.

**3.2. Diffusion and Lifetime Study of the Probes in [Bmim][BF<sub>4</sub>] and [Bmim][PF<sub>6</sub>].** Figure 2 shows the correlation curves of the probes in [Bmim][PF<sub>6</sub>] and [Bmim][BF<sub>4</sub>]. These curves were fitted to a two-component diffusion model as the fits to a single-component diffusion model were found to be unsatisfactory (as judged by the

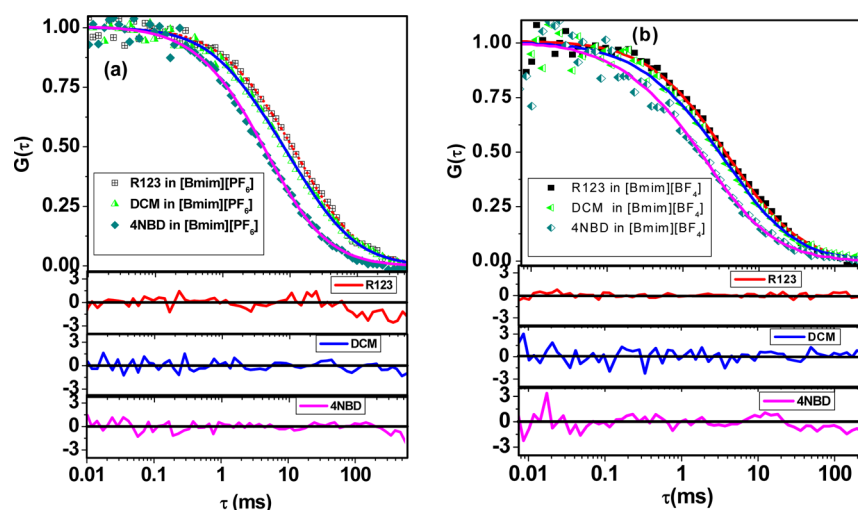


**Figure 2.** Normalized fluorescence correlation curves of the probes in (a) [Bmim][PF<sub>6</sub>] and (b) [Bmim][BF<sub>4</sub>]. The points are the experimental data, and the lines represent best fits to the data considering a two-component diffusion model. The residuals depicting the quality of the fits are shown at the bottom of each panel in the same color.

**Table 2.** Diffusion Parameters of the Probes in [Bmim][PF<sub>6</sub>] and [Bmim][BF<sub>4</sub>]

probe	RTILs <sup>a</sup>	$D_1$ ( $\mu\text{m}^2/\text{s}$ )	$\alpha_1$	$D_2$ ( $\mu\text{m}^2/\text{s}$ )	$\langle D_t \rangle$ ( $\mu\text{m}^2/\text{s}$ )
4NBD	[Bmim][PF <sub>6</sub> ]	$3.4 \pm 0.6$	0.73	$18.0 \pm 3.0$	$7.3 \pm 1.3$
	[Bmim][BF <sub>4</sub> ]	$8 \pm 2$	0.69	$40 \pm 10$	$18.0 \pm 4.5$
DCM	[Bmim][PF <sub>6</sub> ]	$1.30 \pm 0.04$	0.63	$9.6 \pm 3.0$	$4.4 \pm 1.1$
	[Bmim][BF <sub>4</sub> ]	$3.5 \pm 1.0$	0.68	$28.4 \pm 5.0$	$11.5 \pm 2.1$
R123	[Bmim][PF <sub>6</sub> ]	$1.20 \pm 0.03$	0.76	$8.4 \pm 3.0$	$2.94 \pm 0.9$
	[Bmim][BF <sub>4</sub> ]	$3.2 \pm 1.0$	0.62	$20 \pm 5$	$9.6 \pm 2.5$

<sup>a</sup>The viscosities of [Bmim][PF<sub>6</sub>] and [Bmim][BF<sub>4</sub>] are 260 and 90 cP, respectively, at 25 °C.<sup>54</sup>

residuals and  $\chi^2$  values, Figure S2 of the Supporting Information). It is thus evident that all the probes exhibit a bimodal diffusion behavior in both the ionic liquids. The diffusion coefficients for the probes in these ionic liquids, estimated from an average of 50 data sets, are collected in Table 2. The results reveal the following. The fast and slow diffusion coefficients of the molecules differ by a factor of 4–8. The relative contribution of the individual components does not change significantly for 4NBD and DCM, but decreases from 76% to 62% for the slow component of R123 as one moves from [Bmim][PF<sub>6</sub>] to [Bmim][BF<sub>4</sub>]. Another point to note here is that the diffusion of the ionic probe, R123, is slower than that of the neutral probes 4NBD and DCM in both ionic liquids.

Considering the fact that these systems exhibit a single-component diffusion in conventional solvents, the bimodal diffusion behavior of the probes in ionic liquids can perhaps be attributed to the presence of two distinct environments of the RTILs, as indicated in several theoretical and experimental studies in recent years.<sup>9–33</sup> In this context, it is pertinent to note that Guo et al. also observed a similar bimodal diffusion behavior of rhodamine 6G in a series of pyrrolidinium ionic liquids in a recent work.<sup>44</sup> Bhattacharyya and co-workers while studying the diffusion behavior of some fluorescent molecules observed an unusually broad distribution of diffusion coefficient in ionic liquids when compared with that in conventional solvent.<sup>43</sup> Considering these reports, we assign the bimodal diffusion of the molecules to molecular motion in two different regions: domains formed by the alkyl tails and the ionic constituents of the ionic liquids. As the domains formed by the

segregation of the alkyl tails of the ionic liquids are of the order of a few nanometers<sup>18,21,34</sup> and are much smaller than the confocal dimension, while passing through the confocal volume a molecule can pass through both hydrophobic and hydrophilic environments. However, under this situation, one expects a single-component diffusion with the diffusion coefficient equal to the average of the diffusion coefficients in two environments. The observation of two distinct diffusion components (as is the present case) suggests that molecules do not change between two different solvent environments while passing through the observation volume. This is possible when each type of domains is interconnected. A continuity in the domain structure, which is indicated in molecular dynamics simulation studies, allows molecular diffusion only within a given type of environment during the passage through the confocal volume. It is to be noted that Guo et al. offered a similar interpretation to account for their findings.<sup>44</sup> As the size of the aggregated domains of the imidazolium ionic liquids does not change significantly on changing only the anionic component from [PF<sub>6</sub>]<sup>−</sup> to [BF<sub>4</sub>]<sup>−</sup>,<sup>22</sup> it is understandable why the relative contribution of the diffusion components does not change significantly for 4NBD and DCM. On the other hand, a small decrease in the contribution of the slow component of R123 from [Bmim][PF<sub>6</sub>] to [Bmim][BF<sub>4</sub>] is probably due to a stronger association of this probe with the solvent molecules in [Bmim][PF<sub>6</sub>] than in [Bmim][BF<sub>4</sub>].

In order to substantiate the structural origin of these bimodal diffusion behaviors and obtain further insight into this aspect, the fluorescence decay behavior of the probe molecules has been studied in [Bmim][PF<sub>6</sub>] and [Bmim][BF<sub>4</sub>]. Representa-



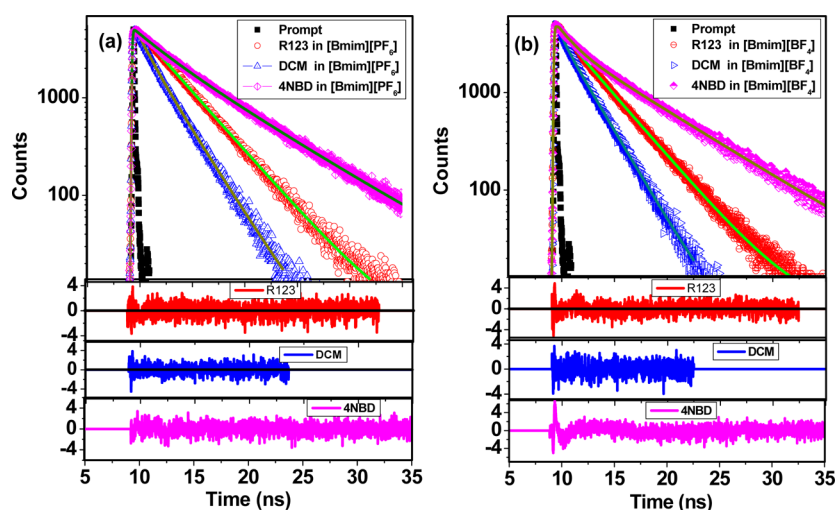


**Figure 3.** Fluorescence decay profile of the probes (a) [Bmim][PF<sub>6</sub>] and (b) [Bmim][BF<sub>4</sub>]. The points are the experimental data, and the lines represent the best fits to the data. The black points (filled square) represent the lamp profile. Except in the case of R123 in [Bmim][PF<sub>6</sub>], all data points are fitted to a biexponential function,  $I(t) = a_1 \exp(-t/\tau_1) + a_2 \exp(-t/\tau_2)$ , where  $a_1$  and  $a_2$  are the pre-exponential factors and  $\tau_1$  and  $\tau_2$  are the lifetime components. Excitation wavelength was 439 nm, and the emission was monitored at 550 nm for R123, 610 nm for 4NBD, and 620 nm for DCM. The residuals depicting the quality of the fits are shown in the lower part of each figure.

tive fluorescence decay profiles of the probes are shown in Figure 3, and the lifetime data are presented in Table 3. A

**Table 3. Time-Resolved Fluorescence Parameters<sup>a</sup> of the Probe Molecules in [Bmim][PF<sub>6</sub>] and [Bmim][BF<sub>4</sub>]**

RTIL	probe	$\tau_1$ ( $a_1$ )	$\tau_2$ ( $a_2$ )	$\langle\tau\rangle^b$
[Bmim][PF <sub>6</sub> ]	R123	—	3.6	3.6
	DCM	1.1 (0.31)	2.6 (0.69)	2.1
	4NBD	1.3 (0.37)	6.2 (0.63)	4.4
[Bmim][BF <sub>4</sub> ]	R123	0.6 (0.18)	3.5 (0.82)	3.0
	DCM	0.6 (0.27)	2.4 (0.73)	2.0
	4NBD	1.4 (0.40)	6.5 (0.60)	4.5

<sup>a</sup>The lifetimes,  $\tau$ , are in nanoseconds. <sup>b</sup> $\langle\tau\rangle$  is defined as  $\langle\tau\rangle = (a_1\tau_1 + a_2\tau_2)/(a_1 + a_2)$ .

biexponential fit to the decay profiles was found to be superior to the single-exponential ones (Supporting Information, Figure S5) except for R123 in [Bmim][PF<sub>6</sub>]. In all cases, the weight of the long-lifetime component is found to be higher, and no significant change in the relative contributions of the decay components is observed in both ionic liquids.

Both 4NBD and DCM are molecular systems, whose fluorescence properties are sensitive to the environment due to the highly polar nature of the emitting state of the molecules.<sup>46,47</sup> Considering the environment sensitive properties of these molecules and the fact that these probes exhibit monoexponential decay in the conventional solvents,<sup>46,47,49</sup> we attribute the biexponential decay behavior of the systems to the heterogeneity in ionic liquids. As these molecular systems possess a short fluorescence lifetime in polar environments, the fast-decay component of DCM and 4NBD can be assigned to molecules from a polar region and the long-lifetime component to molecules from a less polar or nonpolar region. Having assigned the two lifetime components to molecules from the two distinct environments of the ionic liquids, we can use the weight of the two lifetime components to determine the distribution of the molecules into these regions. As the weight of the long-decay component is more than that of the short component, we conclude that DCM and 4NBD are

predominantly distributed in the nonpolar domains formed by the segregation of the alkyl tails. Hence, the slow component of the diffusion, whose contribution is also higher, arises from diffusion in the nonpolar region of the ionic liquids. Considering the literature on the rhodamine dyes,<sup>48,49</sup> we can attribute the long-lifetime component of R123 to molecules from a polar environment and the fast-decay component in [Bmim][BF<sub>4</sub>] to those from a nonpolar region. As the weight of the long-lifetime component is higher for R123, it is evident that this molecule resides predominantly in the polar environments of [Bmim][BF<sub>4</sub>]. On the basis of the above picture, the origin of slow diffusion of R123 compared to the two other probes in these ionic liquids can be understood. As R123 is mainly located in the polar environment, it experiences a strong dragging force due to both hydrogen bonding and electrostatic interaction with the ionic constituents of the ionic liquids. On the other hand, neutral probes, DCM and 4NBD, which reside mainly in the nonpolar region, do not experience any specific or electrostatic interaction with the ionic constituents of the ionic liquids. Thus the lifetime data complements the diffusion data and confirms the structural origin of the microenvironments and the location of the probe molecules in specific regions of the ionic liquids.

**3.2. Diffusion and Lifetime Study of the Probes in Ionic Liquids of Varying Chain Length.** The diffusion behavior of the molecules in a series of [C<sub>n</sub>mim][Tf<sub>2</sub>N] ionic liquids with  $n = 2, 4$ , and  $6$  has been studied to understand the effect of the chain length. Figure 4 shows the correlation curves of the probes in these ionic liquids. Like in earlier cases, the molecules show two-component diffusion dynamics in these ionic liquids as well. The estimated diffusion coefficients and their relative contributions are listed in Table 4. Like in [Bmim][PF<sub>6</sub>] and [Bmim][BF<sub>4</sub>], the diffusion of R123 is found to be slower compared to the neutral probes. In all cases, it is found that the fraction associated with the slow component increases with increasing chain length of the alkyl group.

The bimodal diffusion behavior of the probes in ionic liquids, as described in the previous section, can be interpreted due to the existence of two kinds of solvent environments. Even

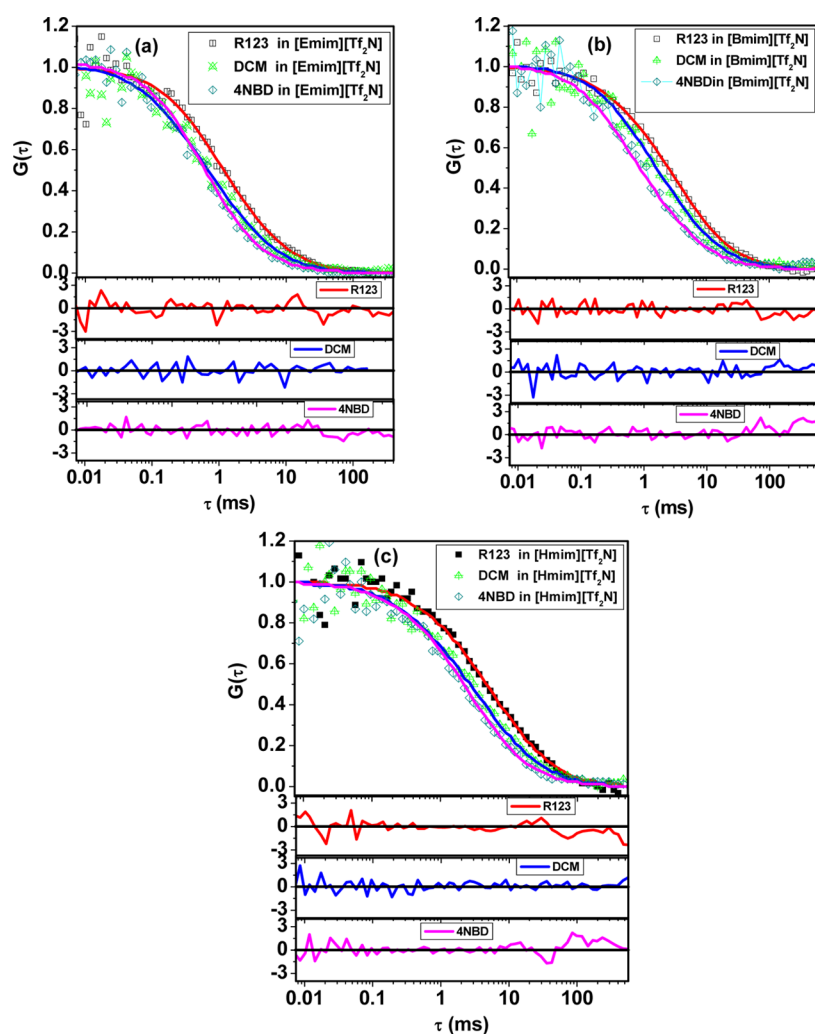


**Figure 4.** Normalized fluorescence correlation curves for the diffusion of the probes (a) [Emim][Tf<sub>2</sub>N], (b) [Bmim][Tf<sub>2</sub>N], and (c) [Hmim][Tf<sub>2</sub>N]. The points are the experimental data, and the lines represent best fits to the data considering a two-component diffusion model. The residuals depicting the quality of the fits are shown at the bottom of each figure in the same color.

**Table 4.** Diffusion Parameters of the Probe Molecules in [Emim][Tf<sub>2</sub>N], [Bmim][Tf<sub>2</sub>N], and [Hmim][Tf<sub>2</sub>N]

probe	RTILs <sup>†</sup>	$D_1$ ( $\mu\text{m}^2/\text{s}$ )	$\alpha_1$	$D_2$ ( $\mu\text{m}^2/\text{s}$ )	$\langle D_t \rangle$ ( $\mu\text{m}^2/\text{s}$ )
R123	[Emim][Tf <sub>2</sub> N]	$7.8 \pm 2.0$	0.39	$28 \pm 8$	$20.1 \pm 5.7$
	[Bmim][Tf <sub>2</sub> N]	$4.5 \pm 1.0$	0.65	$32.6 \pm 5.0$	$14.4 \pm 2.4$
	[Hmim][Tf <sub>2</sub> N]	$3 \pm 0.6$	0.68	$19 \pm 5$	$8.1 \pm 2.0$
DCM	[Emim][Tf <sub>2</sub> N]	$13 \pm 2$	0.43	$50.2 \pm 10$	$34.2 \pm 6.6$
	[Bmim][Tf <sub>2</sub> N]	$5.6 \pm 1.0$	0.54	$38 \pm 4$	$20.5 \pm 2.4$
	[Hmim][Tf <sub>2</sub> N]	$3 \pm 0.6$	0.68	$31.5 \pm 8.0$	$11.8 \pm 3.0$
4NBD	[Emim][Tf <sub>2</sub> N]	$12 \pm 3$	0.29	$49.2 \pm 15$	$38.4 \pm 11.5$
	[Bmim][Tf <sub>2</sub> N]	$9.3 \pm 2.0$	0.47	$44 \pm 10$	$29.3 \pm 6.2$
	[Hmim][Tf <sub>2</sub> N]	$4.5 \pm 1.5$	0.53	$20 \pm 4$	$12.1 \pm 3.0$

<sup>†</sup>The viscosities of [Emim][Tf<sub>2</sub>N], [Bmim][Tf<sub>2</sub>N], and [Hmim][Tf<sub>2</sub>N] are 32, 50, and 67 cP, respectively, at 25 °C.<sup>20,55</sup>

though a slow diffusion of R123 compared to 4NBD is expected based on the hydrodynamic radii of the systems, the slowness of the diffusion of R123 compared to DCM, whose hydrodynamic radius is very similar to that of DCM, can only be explained taking into account the positively charged nature of R123 and its association with the solvent in the polar ionic region. An increase in the fraction of the slow component with increasing chain length is consistent with the results of MD simulation studies and small wide-angle X-ray scattering (SWAXS) experiments, both indicating an increase in the size

of the nonpolar domain formed by the aggregation of the alkyl tail with increasing chain length.<sup>13,14,16,17,21,22,25–27</sup> Perhaps the most surprising result of the present experiments is the observation of a bimodal diffusion behavior of the probes even in small alkyl chain length containing ionic liquid, [Emim]-[Tf<sub>2</sub>N]. This is because the MD simulation studies proposed nanoscale organization in ionic liquids with  $n \geq 4$ .<sup>13,14,16,17</sup> However, recent SWAXS study suggests the existence of the nanoscale structure in [C<sub>n</sub>mim][Tf<sub>2</sub>N] for  $n = 3$  as well.<sup>22</sup>

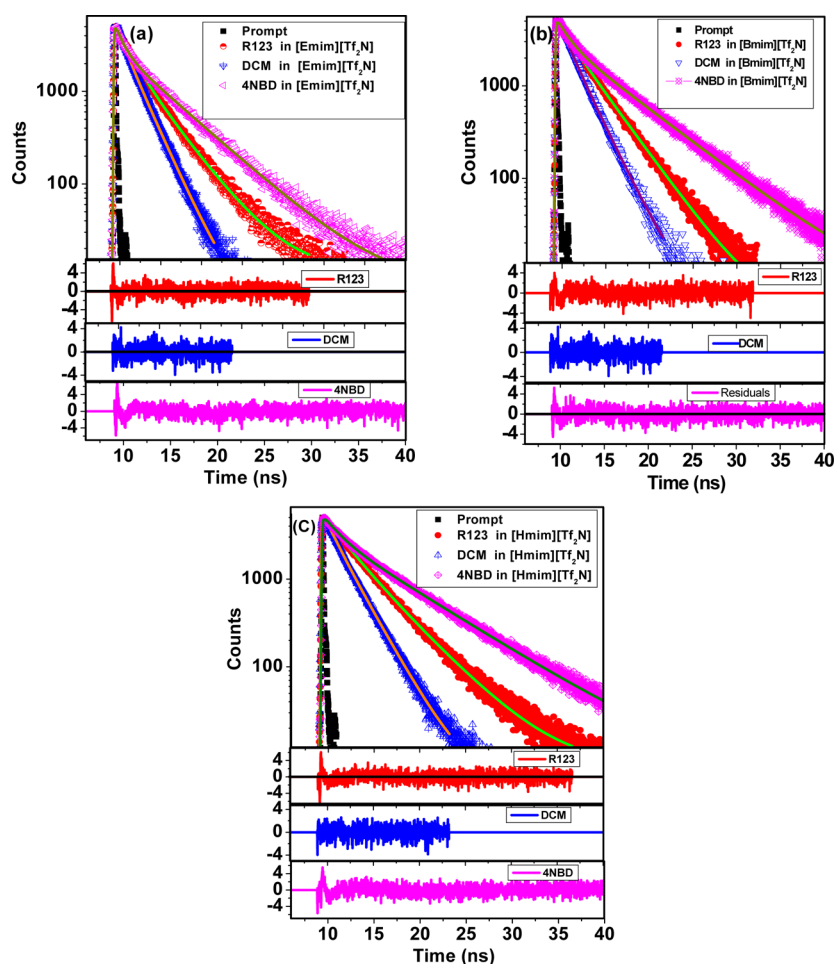


**Figure 5.** Time-resolved fluorescence behavior of the probes in (a) [Emim][Tf<sub>2</sub>N], (b) [Bmim][Tf<sub>2</sub>N], and (c) [Hmim][Tf<sub>2</sub>N]. The points are the experimental data, and the lines represent the best biexponential fits to these data points. Excitation wavelength was 439 nm, and the emission was monitored at 550 nm for R123, 610 nm for 4NBD, and 620 nm for DCM. The residuals depicting the quality of the fits are shown in the lower part of each figure.

Atkin and Warr also observed a low *Q* peak for alkyl ammonium nitrates for *n* = 2 and 3.<sup>23</sup>

In order to confirm these findings, we have studied the fluorescence lifetimes of the molecules in these ionic liquids. The fluorescence decay profiles of all the probes in these ionic liquids have been found to be biexponential with the two lifetime components typical for the respective probes in polar and nonpolar environments. Figure 5 shows the fluorescence decay profiles of the molecules along with the biexponential fits to the data. The fluorescence lifetime data of the systems are collected in Table 5. As can be seen, the short- and long-lifetime components of each molecule do not vary appreciably with the change of the ionic liquids. However, some variation of the weight of the two components can be observed. For DCM, the percentage associated with the long-lifetime component that represents molecules in the nonpolar region exceeds 70% in all cases indicating the preference of this molecule to the nonpolar region of the ionic liquid. For NBD, whose long-lifetime component also represents the molecules residing in the nonpolar region, it increases from 51% in [Emim][Tf<sub>2</sub>N] to 61% in [Hmim][Tf<sub>2</sub>N] indicating the passage of more molecules to the nonpolar region with increase in the alkyl chain length. This observation is consistent with the increase in the size of the nonpolar domain for higher members of the series.<sup>21,22</sup> As far as R123 is concerned, the fraction associated

**Table 5.** Time-Resolved Fluorescence Parameters<sup>a</sup> of the Probes in [Emim][Tf<sub>2</sub>N], [Bmim][Tf<sub>2</sub>N], and [Hmim][Tf<sub>2</sub>N]

RTIL	probe	$\tau_1$ ( <i>a</i> <sub>1</sub> )	$\tau_2$ ( <i>a</i> <sub>2</sub> )	$\langle\tau\rangle^b$
[Emim][Tf <sub>2</sub> N]	R123	1.7 (0.47)	3.6 (0.53)	2.8
	DCM	1.0 (0.21)	2.4 (0.79)	2.1
	4NBD	1.0 (0.49)	5.6 (0.51)	3.3
[Bmim][Tf <sub>2</sub> N]	R123	2.3 (0.39)	3.6 (0.61)	3.1
	DCM	1.0 (0.26)	2.2 (0.74)	1.9
	4NBD	1.3 (0.42)	6.1 (0.58)	4.1
[Hmim][Tf <sub>2</sub> N]	R123	2.4 (0.35)	4.12 (0.65)	3.5
	DCM	1.2 (0.26)	2.4 (0.74)	2.1
	4NBD	1.7 (0.39)	6.8 (0.61)	4.8

<sup>a</sup>The lifetimes,  $\tau$ , are in nanoseconds. <sup>b</sup> $\langle\tau\rangle$  is defined as  $\langle\tau\rangle = (a_1\tau_1 + a_2\tau_2)/(a_1 + a_2)$ .

with the long-lifetime component represents the molecules in the polar environments. This fraction changes from 0.53 in [Emim][Tf<sub>2</sub>N] to 0.65 in [Hmim][Tf<sub>2</sub>N]. This observation can be explained based on the increased hydrophobicity of the nonpolar environment with increasing chain length. As charged molecule R123 prefers to reside in a hydrophilic environment, an increased hydrophobicity of the nonpolar environment enhances the population of the R123 in the polar environment.

Thus, the lifetime study corroborates the presence of two different kinds of environment in these ionic liquids.

#### 4. CONCLUSION

We have studied the translational diffusion of some environment sensitive probe molecules in several ionic liquids using fluorescence correlation spectroscopy technique. Biphasic diffusion dynamics observed for the probes in these media is attributed to the microheterogeneous nature of these media resulting from the segregation of the alkyl chain of the constituents. The presence of polar and nonpolar regions in these ionic liquids is further substantiated by studies on the time-resolved fluorescence decay profiles of the system, which indicate biexponential decay behavior with lifetimes typical of the probes in polar and nonpolar environment. It is shown that a combination of the fluorescence correlation and lifetime techniques can provide useful information on the nature of the microenvironment of the complex media such as the ionic liquids.

#### ■ ASSOCIATED CONTENT

##### ■ Supporting Information

Fluorescence intensity time traces of [Bmim][PF<sub>6</sub>] alone and R123 in [Bmim][PF<sub>6</sub>] (Figure S1); correlation curves fitted to single-component diffusion (SD) model for the probes R123, DCM, and 4NBD in all ionic liquids (Figures S2–S4); fluorescence decay profiles of the probes in all ionic liquids along with single-exponential fits to the data (Figures S5 and S6). This material is available free of charge via the Internet at <http://pubs.acs.org>.

#### ■ AUTHOR INFORMATION

##### Corresponding Author

\*E-mail: [assc@uohyd.ernet.in](mailto:assc@uohyd.ernet.in).

##### Notes

The authors declare no competing financial interest.

#### ■ ACKNOWLEDGMENTS

This work is supported by the J. C. Bose Fellowship (to A.S.) and PURSE Grant (to the University of Hyderabad) of the Department of Science and Technology (DST). S.P. thanks Council of Scientific and Industrial Research (CSIR) for a Fellowship.

#### ■ REFERENCES

- (1) Rogers, R. D.; Seddon, K. R. *Science* **2003**, *302*, 792–793.
- (2) Dupont, J.; de Suja, R. F.; Suarez, P. A. Z. *Chem. Rev.* **2002**, *102*, 3667–3692.
- (3) Wasserscheid, P.; Keim, W. *Angew. Chem., Int. Ed.* **2000**, *39*, 3772–3789.
- (4) Ranu, B. C.; Jana, R. *Eur. J. Org. Chem.* **2006**, 3767–3770.
- (5) Wang, P.; Wenger, B.; Humphry-Baker, R.; Moser, J.-E.; Teuscher, J.; Kantelechner, W.; Mezger, J.; Stoyanov, E. V.; Zakeeruddin, S. M.; Gratzel, M. *J. Am. Chem. Soc.* **2005**, *127*, 6850–6856.
- (6) Kuang, D.; Wang, P.; Ito, S.; Zakeeruddin, S. M.; Gratzel, M. *J. Am. Chem. Soc.* **2006**, *128*, 7732–7733.
- (7) Hallett, J. P.; Welton, T. *Chem. Rev.* **2011**, *111*, 3508–3576.
- (8) Sun, X.; Luo, H.; Dai, S. *Chem. Rev.* **2012**, *112*, 2100–2128.
- (9) Mandal, P. K.; Sarkar, M.; Samanta, A. *J. Phys. Chem. A* **2004**, *108*, 9048–9053.
- (10) Paul, A.; Mandal, P. K.; Samanta, A. *J. Phys. Chem. B* **2005**, *109*, 9148–9153.
- (11) Skrzypczak, A.; Neta, P. *J. Phys. Chem. A* **2003**, *107*, 7800–7803.
- (12) Tokuda, H.; Hayamizu, K.; Ishii, K.; Susan, M. A. B. H.; Watanabe, M. *J. Phys. Chem. B* **2005**, *109*, 6103–6110.
- (13) Wang, Y.; Voth, G. A. *J. Am. Chem. Soc.* **2005**, *127*, 12192–12193.
- (14) Wang, Y.; Voth, G. A. *J. Phys. Chem. B* **2006**, *110*, 18601–18608.
- (15) Hu, Z.; Margulis, C. J. *Proc. Natl. Acad. Sci. U.S.A.* **2006**, *103*, 831–836.
- (16) Lopes, J. N. C.; Padua, A. A. H. *J. Phys. Chem. B* **2006**, *110*, 3330–3335.
- (17) Lopes, J. N. C.; Costa Gomes, M. F.; Padua, A. A. H. *J. Phys. Chem. B* **2006**, *110*, 16816–16818.
- (18) Iwata, K.; Okajima, H.; Saha, S.; Hamaguchi, H. *Acc. Chem. Res.* **2007**, *40*, 1174–1181.
- (19) Paul, A.; Samanta, A. *J. Phys. Chem. B* **2007**, *111*, 1957–1962.
- (20) Paul, A.; Samanta, A. *J. Phys. Chem. B* **2008**, *112*, 16626–16632.
- (21) Triolo, A.; Russina, O.; Bleif, H.-J.; Di Cola, E. *J. Phys. Chem. B* **2007**, *111*, 4641–4644.
- (22) Russina, O.; Triolo, A.; Gontrani, L.; Caminiti, R.; Xiao, D.; Hines, L. G., Jr.; Bartsch, R. A.; Quitevis, E. L.; Plechkova, N.; Seddon, K. R. *J. Phys.: Condens. Matter* **2009**, *21*, 424121/1–9.
- (23) Atkin, R.; Warr, G. G. *J. Phys. Chem. B* **2008**, *112*, 4164–4166.
- (24) Hayes, R.; Imberti, S.; Warr, G. G.; Atkin, R. *Phys. Chem. Chem. Phys.* **2011**, *13*, 3237–3247.
- (25) Russina, O.; Triolo, A.; Gontrani, L.; Caminiti, R. *J. Phys. Chem. Lett.* **2012**, *3*, 27–33.
- (26) Russina, O.; Triolo, A. *Faraday Discuss.* **2012**, *154*, 97–109.
- (27) Macchiagodena, M.; Gontrani, L.; Ramondo, F.; Triolo, A.; Caminiti, R. *J. Chem. Phys.* **2011**, *134*, 114521/1–15.
- (28) Funston, A. M.; Fadeeva, T. A.; Wishart, J. F.; Castner, E. W., Jr. *J. Phys. Chem. B* **2007**, *111*, 4963–4977.
- (29) Fruchey, K.; Fayer, M. D. *J. Phys. Chem. B* **2010**, *114*, 2840–2845.
- (30) Arzhantsev, S.; Jin, H.; Baker, G. A.; Maroncelli, M. *J. Phys. Chem. B* **2007**, *111*, 4978–4989.
- (31) Fruchey, K.; Lawler, C. M.; Fayer, M. D. *J. Phys. Chem. B* **2012**, *116*, 3054–3064.
- (32) Jin, H.; Li, X.; Maroncelli, M. *J. Phys. Chem. B* **2007**, *111*, 13473–13478.
- (33) Adhikari, A.; Sahu, K.; Dey, S.; Ghosh, S.; Mandal, U.; Bhattacharyya, K. *J. Phys. Chem. B* **2007**, *111*, 12809–12816.
- (34) Yoshida, K.; Iwata, K.; Nishiyama, Y.; Kimura, Y.; Hamaguchi, H. *J. Chem. Phys.* **2012**, *136*, 104504/1–8.
- (35) Hardacre, C.; Holbrey, J. D.; Mullan, C. L.; Youngs, T. G. A.; Bowron, D. T. *J. Chem. Phys.* **2010**, *133*, 074510/1–7.
- (36) Annappureddy, H. V. R.; Kashyap, H. K.; De Biase, P. M.; Margulis, C. J. *J. Phys. Chem. B* **2010**, *114*, 16838–16846.
- (37) Lackowicz, J. R. *Principles of Fluorescence Spectroscopy*; Springer: New York, 2006; Chapter 24.
- (38) Al-Soufi, W.; Reija, B.; Novo, M.; Felekyan, S.; Kuhnemuth, R.; Seidel, C. A. M. *J. Am. Chem. Soc.* **2005**, *127*, 8775–8784.
- (39) Rochira, J. A.; Gudheti, M. V.; Gould, T. J.; Laughlin, R. R.; Nadeau, J. L.; Hess, S. T. *J. Phys. Chem. C* **2007**, *111*, 1695–1708.
- (40) Haupts, U.; Maiti, S.; Schwill, P.; Webb, W. W. *Proc. Natl. Acad. Sci. U.S.A.* **1998**, *95*, 13573–13578.
- (41) Chattopadhyay, K.; Saffarian, S.; Elson, E. L.; Frieden, C. *Biophys. J.* **2005**, *88*, 1413–1422.
- (42) Werner, J. H.; Baker, S. N.; Baker, G. A. *Analyst* **2003**, *128*, 786–789.
- (43) Sasmal, D. K.; Mandal, A. K.; Mondal, T.; Bhattacharyya, K. *J. Phys. Chem. B* **2011**, *115*, 7781–7787.
- (44) Guo, J.; Baker, G. A.; Hillesheim, P. C.; Dai, S.; Shaw, R. W.; Mahurin, S. M. *Phys. Chem. Chem. Phys.* **2011**, *13*, 12395–12398.
- (45) Sarkar, A.; Ali, M.; Baker, G. A.; Tetin, S. Y.; Ruan, Q.; Pandey, S. *J. Phys. Chem. B* **2009**, *113*, 3088–3098.
- (46) Saha, S.; Samanta, A. *J. Phys. Chem. A* **1998**, *102*, 7903–7912.
- (47) Mialocq, J. C.; Meyer, M. *Laser Chem.* **1990**, *10*, 277–296.
- (48) Lopez Arbeloa, L.; Lopez Arbeloa, F.; Tapia Estevej, M. J.; Lopez Arbeloa, I. *J. Phys. Chem.* **1991**, *95*, 2203–2208.



- (49) Chowdhury, S. A.; Lim, M. *Bull. Korean Chem. Soc.* **2011**, *32*, 583–589.
- (50) Perrin, D. D.; Armarego, W. L. F.; Perrin, D. R. *Purification of Laboratory Chemicals*; Pergamon Press: New York, 1980.
- (51) Wahl, M. Technical note, PicoQuant GmbH, 2004; pp 1–6.
- (52) Mahurin, S. M.; Dai, S.; Barnes, M. D. *J. Phys. Chem. B* **2003**, *107*, 13336–13340.
- (53) Petrasek, Z.; Schwille, P. *Biophys. J.* **2008**, *94*, 1437–1448.
- (54) Santhosh, K.; Banerjee, S.; Rangaraj, N.; Samanta, A. *J. Phys. Chem. B* **2010**, *114*, 1967–1974.
- (55) Widegren, J. A.; Magee, J. W. *J. Chem. Eng. Data* **2007**, *52*, 2331–2338.
- (56) Aki, S. N. V. K.; Brennecke, J. F.; Samanta, A. *Chem. Commun.* **2001**, 413–414.
- (57) Karmakar, R.; Samanta, A. *J. Phys. Chem. A* **2002**, *106*, 6670–6675.
- (58) Karmakar, R.; Samanta, A. *J. Phys. Chem. A* **2003**, *107*, 7340–7346.
- (59) Weingartner, H. *Angew. Chem., Int. Ed.* **2008**, *47*, 654–670.
- (60) Edward, J. T. *J. Chem. Educ.* **1970**, *47*, 261–270.